Simulation study of high-reverse blocking AlGaN/GaN power rectifier with an integrated lateral composite buffer diode

Zeheng Wang ✉, *Fangzhou Wang, Songnan Guo, Zirui Wang*

School of Microelectronics and Soild-State Electronics, University of Electronic Science and Technology of China, Chengdu, 610054, People's Republic of China

✉ *E-mail: zen.w@foxmail.com*

Published in Micro & Nano Letters; Received on 2nd February 2017; Revised on 3rd April 2017; Accepted on 11th April 2017

In this study, a novel AlGaN/GaN power rectifier with an integrated lateral composite buffer diode (IBD-Rectifier) for reverse blocking capability improvement is proposed and investigated by Sentaurus simulations (this paper includes only simulated data and no real experimental result). AlGaN buffer layer under the anode is adopted to realise great high reverse blocking capability. A minimum turn-on voltage of 0.6 V and a maximum breakdown voltage (BV) >1.3 kV are simultaneously obtained in the IBD-Rectifier, resulting in a high Baliga's figure of merits $BV^2/R_{on,sp}$ ($R_{on,sp}$ is specific-on resistance) of ∼3000 MW/cm^2. In comparison with MIS-gated hybrid anode diode and conventional schottky barrier diode, the IBD-Rectifier delivers an excellent theoretical method to achieve superior performances in high-efficiency GaN power applications.

1. Introduction: The III–V semiconductors are capable to be applied in high-efficiency power electronics because of their high-electron mobility, high-critical electric field, and wide bandgap [1–5]. Among the power rectifiers based on III–V semiconductor materials, AlGaN/GaN power rectifier are promising candidates to meet the demands of next generation high-power applications [6]. Rectifiers with low-turn-on voltage (V_T) and high-breakdown voltage (BV) are required for minimising the static power consumption [7]. High V_T and low BV are two major limitations of conventional schottky barrier diode (conv. SBD). In recent years, tremendous efforts have been made on developing novel structures and optimising the performances of AlGaN/GaN power diodes [8–20]. Meanwhile, great attention has been attracted to replace GaN with AlGaN as a buffer layer in order to obtain a high BV, which has been demonstrated in HEMTs [21].

To further improve the BV, a novel high-reverse blocking AlGaN/GaN power rectifier with an integrated lateral composite buffer diode (IBD-Rectifier) is reported and investigated by Sentaurus simulations (this paper includes only simulated data and no real experimental result). AlGaN buffer layer under the anode leads to a normally-off state because the polarisation charge density at AlGaN-barrier/AlGaN-buffer interface is reduced. AlGaN buffer which has the wider bandgap contributes to the enhancement of the BV. Meanwhile, anode consisting of ohmic contact and metal-isolator-semiconductor (MIS) structure ensures a low V_T. Thus, AlGaN/GaN lateral composite buffer layer is designed as an integrated diode. A minimum V_T of 0.6 V and a maximum BV >1.3 kV are achieved. Therefore, the proposed IBD-Rectifier with a high Baliga's figure of merits (BFOM) $BV^2/R_{on,sp}$ ($R_{on,sp}$ is specific-on resistance) of ∼3000 MW/cm^2 provides with an excellent theoretical method to cater for the demands of high-efficiency GaN power applications.

2. Structures and models: Fig. 1*a* is the schematic cross section of the IBD-Rectifier structure model in simulations. The IBD-Rectifier features that AlGaN material is used as the buffer layer under the anode. The hetero-structures consist of a 25 nm $Al_{0.3}Ga_{0.7}N$ barrier layer, a 1 μm GaN buffer layer and 1 μm AlGaN buffer layer. The Al content of AlGaN buffer layers (X_B) is 0.13, 0.14, and 0.15, respectively. A 50 nm nitride layer and a 10 nm HfO_2 dielectric layer are also included. The IBD-Rectifier is able to be modified as an enhancement-mode transistor in the future. As comparison, MIS-gated hybrid anode diode (MG-HAD) which has been reported in [11] and conv. SBD are built as shown in Figs. 1*b* and *c*, respectively. In addition, metal work function and area factor are 5.1 eV and 1000 in simulations, respectively. The line A and the two-dimensional-electron-gas (2DEG) channel are also marked for future function (X-coordinate and Y-coordinate are given in Fig. 1). Acceptor-like traps at three interfaces of hetero-structures are also taken into consideration. A sheet density of 5×10^{12} cm^{-2} and an activation energy of 0.7 eV with respect to the conduction band minimum (E_C) are adopted by referencing [22, 23]. Meanwhile, it has been demonstrated that AlGaN buffer layer has relative worse crystal quality because of its high Al composition [24]. Thus, the amount of the traps in AlGaN buffer layer (8×10^{16} cm^{-3}, $E_C - 1.5$ eV) is larger than GaN buffer layer (4×10^{16} cm^{-3}, $E_C - 1.3$ eV) in simulations. Material parameters of AlN and GaN are needed for input file. The material parameters provided by Sentaurus material database include lattice parameters, piezoelectric polarisation settings, dielectric constants, lattice heat capacity, thermal conductivity, hydro parameters, bandgap, mobility models, and recombination/generation models. The lattice mismatch generated by strain relaxation of materials could lead to a reduction of polarisation charges. In piezoelectric polarisation settings, strain relaxation degree of 0.2 is adopted to simulate the lattice mismatch of the hetero-interface [25]. AlGaN material settings are able to be proportionally calculated by the quantities of AlN and GaN.

At the interfaces of heterojunction, the total polarisation charge σ is given as follows [25]

$$\sigma = P_{SP}(\text{Buffer}) - P_{SP}(\text{Barrier}) + P_{PZ}(\text{Buffer}) - P_{PZ}(\text{Barrier}) \quad (1)$$

where P_{SP}(Barrier) and P_{SP}(Buffer) are the spontaneous polarisation degrees, P_{PZ}(Barrier) and P_{PZ}(Buffer) are the piezoelectric polarisation degrees. The interface of two kinds of buffer layers is not affected by polarisation-induced charges since the direction of this hetero-interface is perpendicular to the polarisation direction [26, 27]. E_C profiles along the line A (the line A is marked in Fig. 1*a*.) in IBD-Rectifiers are illustrated in Fig. 2. E_C is higher than the Fermi level (E_F) under the forward voltage (V_F) of 0 V.

© The Institution of Engineering and Technology 2017
Micro & Nano Letters, 2017, Vol. 12, Iss. 9, pp. 660–663
doi: 10.1049/mnl.2017.0057

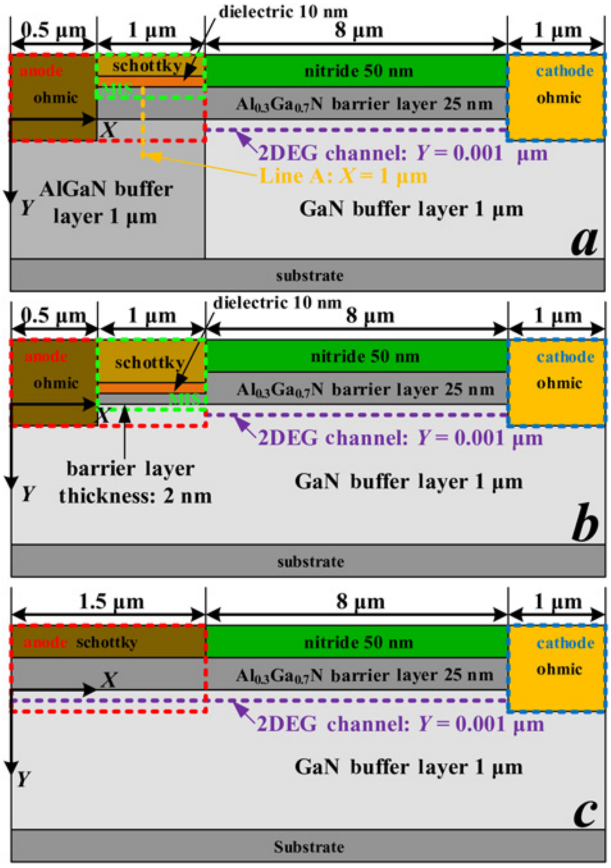

Fig. 1 *Structure schematics of the simulation models with cathode-anode distance of 8 µm*
a IBD-Rectifier
b MIS-gated hybrid anode diode (MG-HAD)
c Conventional SBD (Conv. SBD)

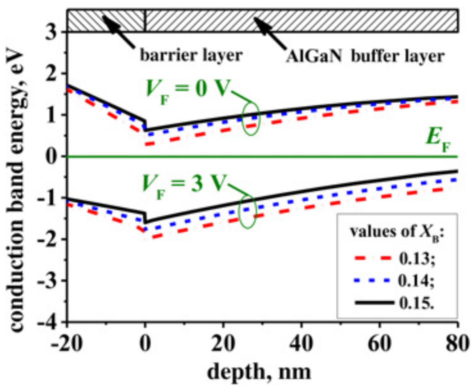

Fig. 2 *E_C profiles along the line A in the IBD-Rectifier with $V_F = 0$ V and 3 V*

Different X_B corresponds to different E_C distributions, which is caused by different polarisation degrees. For high X_B devices, E_C at the interface of barrier/buffer is higher than that of devices with low X_B because of the relative poor polarisation effect. When applied V_F exceeds the threshold voltage of the AlGaN-barrier/AlGaN-buffer interface, E_C begins to fall below the E_F and the device turns to on-state.

3. Results and discussions: The simulated forward characteristics are plotted in Fig. 3. The V_T is defined as the V_F when the forward current reaches 1 mA/mm. The simulated V_T of the

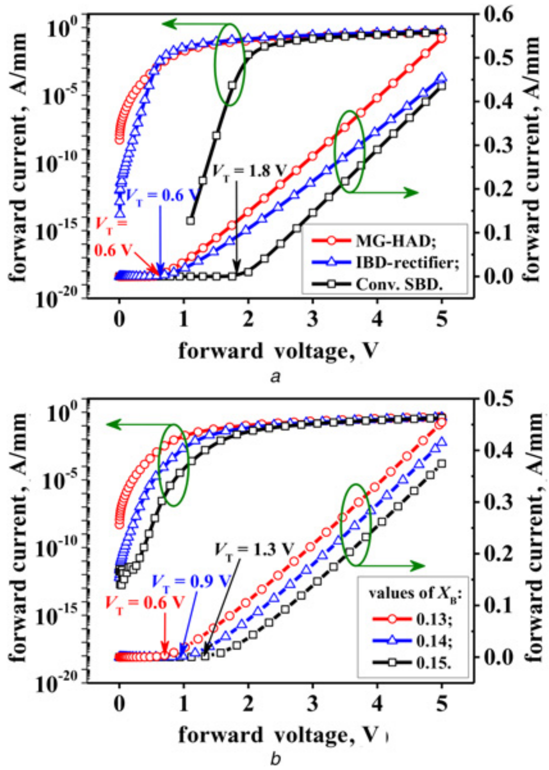

Fig. 3 *Forward characteristics*
a Compared devices and the IBD-Rectifier with $X_B = 0.13$
b IBD-Rectifiers with different X_B

MG-HAD (0.6 V) is in agreement with the experimental data [11]. Turn-on voltages of the IBD-Rectifiers are obtained as follows: 0.6, 0.9 and 1.3 V. V_T of the IBD-Rectifier is determined by the threshold voltage of the AlGaN-barrier/AlGaN-buffer interface and could be modulated by changing X_B. E_C profiles along 2DEG channel are illustrated in Fig. 4. E_C of 2DEG channel in the MG-HAD is lower than that of the other two devices when applying V_F, resulting in a relative higher forward current. It is worth noting the depth of the 2DEG channel E_C in MG-HAD and the IBD-Rectifier with $X_B = 0.13$ is closed, which reveals the IBD-Rectifier devices have satisfying forward performance as good as MG-HAD.

Fig. 5 demonstrates the 2DEG channel E_C distribution of the IBD-Rectifiers around buffer-buffer hetero-interface, together with the equivalent circuit of the IBD-Rectifier. AlGaN/GaN lateral composite buffer layer is designed as an integrated diode. A low V_F makes this diode turn to on-state. When applying high reverse voltage (V_R), the integrated diode holds the most reverse voltage and the device will be disabled just once its breakdown.

The simulated reverse characteristics are illustrated in Fig. 6. The *BV* is defined as the V_R when the reserve current reaches 10 µA/mm. *BVs* are obtained as follows: 60, 510 1320, 1700 and 1830 V. The *BV* of MG-HAD is calibrated by referencing the experimental data [11], *BV*s (@10 µA/mm) of MG-HAD with cathode-anode distance of 5 and 10 µm are ∼430 and 850 V, respectively). In this Letter, cathode–anode distance of 8 µm is adopted to ensure the convergence of the calculation. High *BV*s (>1.3 kV) of the IBD-Rectifiers is superior than that of MG-HAD and conv. SBD. Electric field distribution profiles along the 2DEG channel at *BVs*, electrostatic potential distributions at *BVs*, and the total current density distributions with $V_R = 500$ V are shown in Figs. 7–9, respectively. The reverse blocking of the IBD-Rectifier is dominated by the leakage current between the two ohmic contacts through GaN buffer that bypassing the well depleted channel. Compared with GaN material, AlGaN material which has

© The Institution of Engineering and Technology 2017

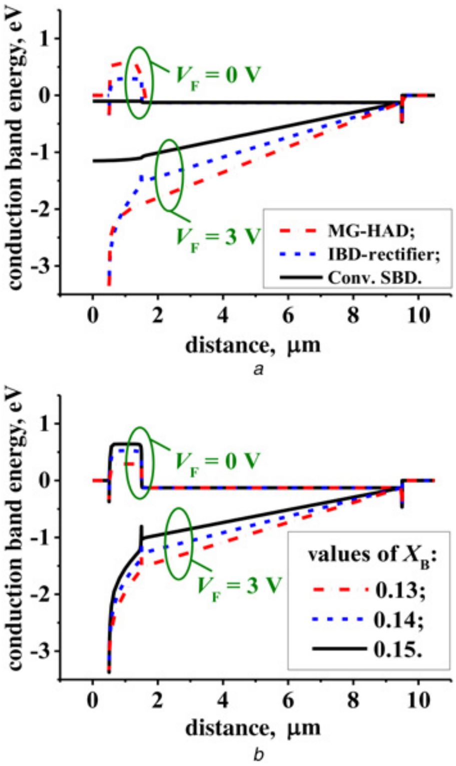

Fig. 4 *E_C profiles along the 2DEG channel*
a Compared devices and the IBD-Rectifier with $X_B = 0.13$
b IBD-Rectifiers with different X_B

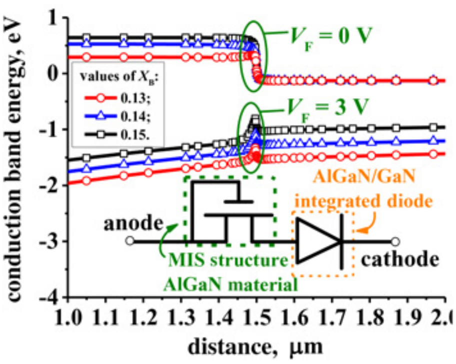

Fig. 5 *E_C profiles along the 2DEG channel in IBD-Rectifiers around buffer-buffer hetero-interface*

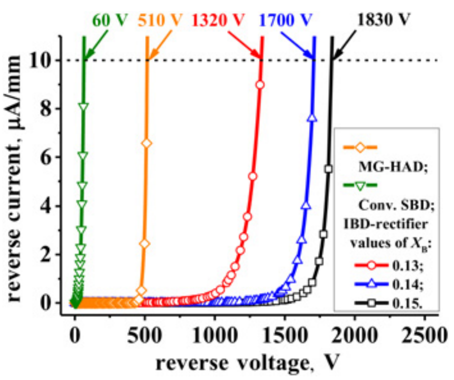

Fig. 6 *Reverse characteristics*

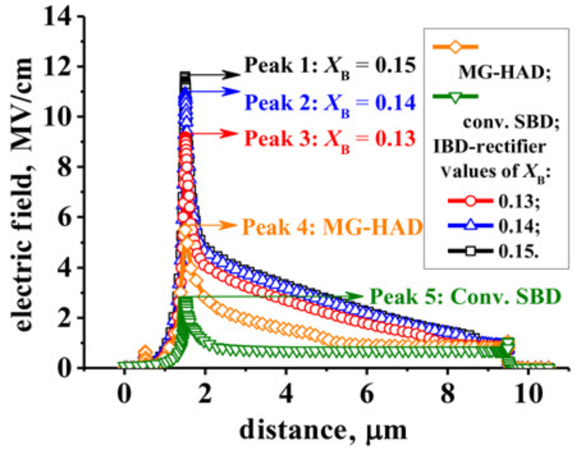

Fig. 7 *Electric field distribution profiles along the 2DEG channel at BVs*

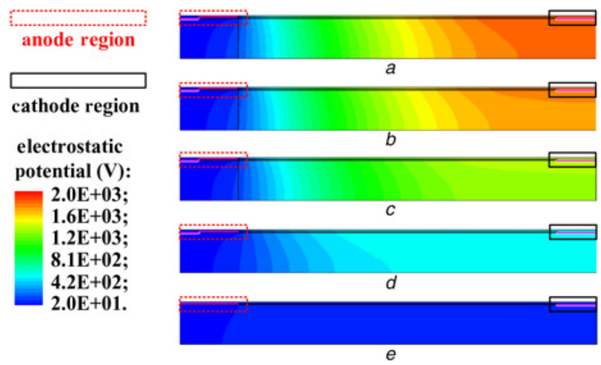

Fig. 8 *Electrostatic potential distribution at BVs*
a IBD-Rectifier with $X_B = 0.15$
b IBD-Rectifier with $X_B = 0.14$
c IBD-Rectifier with $X_B = 0.13$
d MG-HAD
e Conv. SBD

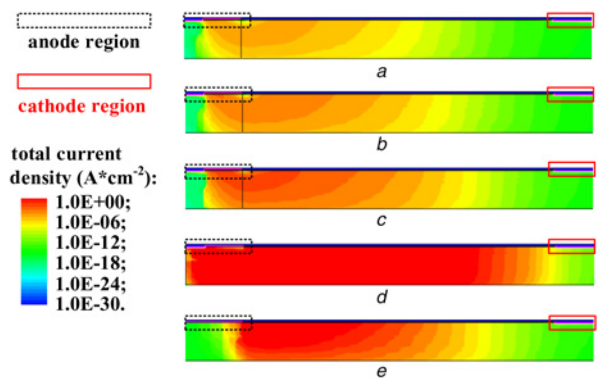

Fig. 9 *Total current density with reverse voltage of 500 V*
a IBD-Rectifier with $X_B = 0.15$
b IBD-Rectifier with $X_B = 0.14$
c IBD-Rectifier with $X_B = 0.13$
d MG-HAD
e Conv. SBD

wider bandgap leads to the lower carrier density. As a result, the width of depletion region is longer in the IBD-Rectifier when applying high V_R. The extension of the depletion region contributes to suppress the leakage current, significantly reducing the electrostatic potential sharply and increasing the breakdown electric field peak around cathode-side anode edge. A higher V_R is required to reach

© The Institution of Engineering and Technology 2017

breakdown criteria (10 µA/mm) in the IBD-Rectifiers. For the IBD-Rectifier with higher X_B, AlGaN buffer with wider bandgap further suppresses the leakage current meanwhile makes an enhancement on *BV*. Therefore, the reverse blocking capability of the IBD-Rectifiers is significantly improved.

The IBD-Rectifier achieves a maximum BFOM of ~3000 MW/cm^2, which means that the IBD-Rectifier with low V_T and high *BV* shows great potential in high efficiency GaN power applications. The fabrication of the IBD-Rectifier could be realised by referencing metal organic chemical vapour deposition selective growth technique [28, 29] in the future.

4. Conclusion: A novel high-reverse blocking AlGaN/GaN power rectifier with an IBD-Rectifier is presented and investigated by Sentaurus simulations (this paper includes only simulated data and no real experimental result). The IBD-Rectifier has a high BV (>1.3 kV) meanwhile a low turn-on voltage as low as 0.6 V in simulations. A maximum BFOM $BV^2/R_{\mathrm{on,sp}}$ ($R_{\mathrm{on,sp}}$ is specific-on resistance) of ~3000 MW/cm^2 is achieved. The results demonstrate a new theoretical method to realise a low turn-on voltage and great high reverse blocking by integrating a lateral composite buffer diode, which is capable to be applied for designing high efficiency GaN power devices prospectively.

5 References

[1] Al-Douri Y.: 'Electronic and positron properties of zinc-blende structure of GaN, AlN, and their alloy $Ga_{1-x}Al_xN$', *J. Appl. Phys.*, 2003, **93**, (12), pp. 9730–9736

[2] Ahmed N.M., Ramizy A., Hassan Z., *et al.*: 'Nano and micro porous GaN characterization using image processing method', *Optik*, 2012, **123**, (12), pp. 1074–1078

[3] Al-Douri Y.: 'Optical properties of GaN nanostructures for optoelectronic applications', *Procedia Eng.*, 2013, **53**, (7), pp. 400–404

[4] Baaziz H., Charifi Z., Reshak A.H., *et al.*: 'Structural and electronic properties of GaN_xAs_{1-x} alloys', *Appl. Phys. A: Mater. Sci. Process.*, 2012, **106**, (3), pp. 687–696

[5] Bouhemadou A., Haddadi K., Bin-Omran S., *et al.*: 'Structural, elastic, electronic and optical properties of the quaternary nitridogallate $LiCaGaN_2$: First-principles study', *Mater. Sci. Semicond. Process.*, 2015, **40**, pp. 64–76

[6] Millan J.: 'Wide band-gap power semiconductor devices', *Circuits Devices Syst. Lett.*, 2007, **1**, (2), pp. 372–379

[7] Tsou C.W., Wei K.P., Lian Y.W., *et al.*: '2.07-kV AlGaN/GaN schottky barrier diodes on silicon with high Baliga's figure-of-merit', *IEEE Electron Device Lett.*, 2016, **37**, (1), pp. 70–73

[8] Chen W., Wong K., Huang W., *et al.*: 'High-performance AlGaN/GaN lateral field-effect rectifiers compatible with high electron mobility transistors', *Appl. Phys. Lett.*, 2008, **92**, (25), pp. 253501-1–253501-3

[9] Wang Z., Zhang B., Chen W., *et al.*: 'A novel hybrid-anode AlGaN/GaN field-effect rectifier with low operation voltage'. 2010 10th IEEE Int. Conf. on Solid-State and Integrated Circuit Technology (ICSICT), Shanghai, China, 2010, pp. 1889–1891

[10] Lee J., Park B., Cho C., *et al.*: 'Low turn-on voltage AlGaN/GaN-on-Si rectifier with gated ohmic anode', *IEEE Electron Device Lett..*, 2013, **34**, (2), pp. 214–216

[11] Zhou Q., Jin Y., Shi Y., *et al.*: 'High reverse blocking and low onset voltage AlGaN-GaN-on-Si lateral power diode with MIS-gated hybrid anode', *IEEE Electron Device Lett..*, 2015, **36**, (7), pp. 660–662

[12] Matioli E., Lu B., Palacios T.: 'Ultralow leakage current AlGaN/GaN schottky diodes with 3-D anode structure', *IEEE Trans. Electron Devices*, 2013, **60**, (10), pp. 3365–3370

[13] Zhu M.D., Song B., Qi M., *et al.*: '1.9-kV AlGaN/GaN lateral schottky barrier diodes on silicon', *IEEE Electron Device Lett..*, 2015, **36**, (4), pp. 375–377

[14] Lenci S., Jaeger B.D., Carbonell L., *et al.*: 'Au-free AlGaN/GaN power diode on 8-in Si substrate with gated edge termination', *IEEE Electron Device Lett..*, 2013, **34**, (8), pp. 1035–1037

[15] Lian Y., Lin Y., Yang J., *et al.*: 'AlGaN/GaN schottky barrier diodes on silicon substrates with selective Si diffusion for low onset voltage and high reverse blocking', *IEEE Electron Device Lett..*, 2013, **34**, (8), pp. 981–983

[16] Li G., Liu H., Chyi J.: 'High-performance AlGaN/GaN schottky diodes with an AlGaN/AlN buffer layer', *IEEE Electron Device Lett..*, 2011, **32**, (11), pp. 1519–1521

[17] Lee H., Jung D.Y., Park Y., *et al.*: '0.34 V_T AlGaN/GaN-on-Si large schottky barrier diode with recessed dual anode metal', *IEEE Electron Device Lett..*, 2015, **36**, (11), pp. 1132–1134

[18] Treidel E.B., Hilt O., Wentzel A., *et al.*: 'Fast GaN based schottky diodes on Si(111) substrate with low onset voltage and strong reverse blocking', *Phys. Status Solidi*, 2013, **10**, (5), pp. 849–852

[19] Zhou Q., Wang L., Bao X., *et al.*: 'High performance AlGaN/GaN power diode with edge-terminated hybrid anode'. 2014 12th IEEE Int. Conf. on Solid-State and Integrated Circuit Technology (ICSICT), Guilin, China, 2014, pp. 1–3

[20] Treidel E.B., Hilt O., Zhytnytska R., *et al.*: 'Fast-switching GaN-based lateral power schottky barrier diodes with low onset voltage and strong reverse blocking', *IEEE Electron Device Lett..*, 2012, **33**, (3), pp. 357–359

[21] Raman A., Dasgupta S., Rajan S., *et al.*: 'AlGaN channel high electron mobility transistors: Device performance and power-switching figure of merit', *Jpn. J. Appl. Phys.*, 2008, **47**, (47), pp. 3359–3361

[22] Tang Z., Huang S., Tang X., *et al.*: 'Influence of AIN passivation on dynamic on-resistance and electric field distribution in high-voltage AlGaN/GaN-on-Si HEMTs', *IEEE Trans. Electron Devices*, 2014, **61**, (8), pp. 2785–2792

[23] Fang Z.Q., Claflin B., Look D.C., *et al.*: 'Deep traps in AlGaN/GaN heterostructures studied by deep level transient spectroscopy: Effect of carbon concentration in GaN buffer layers', *J. Appl. Phys.*, 2010, **108**, (6), pp. 063706-1–063706-6

[24] Ha W., Zhang J., Zhao S., *et al.*: 'AlGaN channel high electron mobility transistors with ultra-low drain-induced-barrier-lowering coefficient', *Chin. Phys. Lett.*, 2013, **30**, (12), pp. 127201-1–127201-3

[25] Wang Z., Zhang B., Chen W., *et al.*: 'A closed-form charge control model for the threshold voltage of depletion- and enhancement-mode AlGaN/GaN devices', *IEEE Trans. Electron Devices*, 2013, **60**, (5), pp. 1607–1612

[26] Kuroda M., Ueda T., Tanaka T.: 'Nonpolar AlGaN/GaN metal–insulator-semiconductor heterojunction field-effect transistors with a normally off operation', *IEEE Trans. Electron Devices*, 2010, **57**, (2), pp. 368–372

[27] Fujiwara T., Keller S., Speck J.S., *et al.*: 'Low ohmic contact resistance m-plane AlGaN/GaN heterojunction field-effect transistors with enhancement-mode operations', *Appl. Phys. Express*, 2010, **3**, (10), pp. 101002-1–101002-3

[28] Liu Z.J., Huang T., Ma J., *et al.*: 'Monolithic integration of AlGaN/GaN HEMT on LED by MOCVD', *IEEE Electron Device Lett..*, 2014, **35**, (3), pp. 330–332

[29] Liu C., Cai Y., Zou X., *et al.*: 'Low-leakage high-breakdown laterally integrated HEMT-LED via n-GaN electrode', *IEEE Photonics Technol. Lett.*, 2016, **28**, (10), pp. 1130–1133

© The Institution of Engineering and Technology 2017